Iranian Journal of Science & Technology, Transaction A, Vol. 29, No. A3
Printed in The Islamic Republic of Iran, 2005

ON THE INVESTIGATION OF SPARK FORMATION CONDITIONS AND ENERGY GAIN IN INERTIAL CONFINEMENT FUSION *

A. GHASEMIZAD[1**], M. R. ESKANDARI[2], S. KHOSHBINFAR[1] AND M. KAMRAN[1]

[1]Department of Physics, Faculty of Science, University of Guilan, Rasht, I. R. of Iran,
Email: ghasemi@guilan.ac.ir
[2]Department of Physics, Shiraz University, Shiraz, I. R. of Iran
Email: eskandari@physics.susc.ac.ir

Abstract – In isobaric models for inertial confinement fusion it is assumed that the target configuration at stagnation time (maximum compression) consists of two regions, hot spark and cold fuel, respectively. Here the conditions of spark formation and ignition in hydrogen equimolar isotopes in central spark ignition are investigated and permissible values of H_s and T_s are evaluated numerically. By introducing a dimensionless parameter, ψ_s, the class of targets are considered by the specific value of ψ_s. Finally, limiting fuel energy gain curve (G_f*) as a function of ignition energy (E_{ign}) allows different implosion velocities to be calculated. This result is in good agreement with more complex hydrodynamic models.

Keywords – Central spark ignition, spark parameter, isobaric model, limiting gain curve

1. INTRODUCTION

Vast efforts have been taken to achieve a generation of energy from controlled nuclear fusion both in magnetic confinement fusion (MCF) and inertial confinement fusion (ICF) [1, 2]. ICF is an approach to fusion that relies on the inertia of the fuel mass to provide confinement [3-5]. It is based on micro explosion of thermonuclear targets.

$$D + T \rightarrow \alpha + n + 17.6\,MeV \tag{1}$$

A major challenge has always been to come up with a target design that would be appropriate for energy production [6], i.e. a major scientific requirement for using ICF is to reach high energy gain G_f [4, 7, 8]:

$$G_f = E_{TN} / E_f \tag{2}$$

where E_{TN} is thermonuclear energy released from a deuterium-tritium (DT) fusion reaction that is carried with fusion products, and E_f is the fraction of incident beam, converted to fuel thermal energy. Central spark ignition, which is currently being considered as a scheme for reaching high energy gain, is required to drive fuel to lower specific entropy than its inner part by a suitable set of shocks and refraction during shell implosion. In this concept, ignition occurs at the fuel center and then propagates burning waves to the surrounding dense and cold fuel layer. For this, certain

*Received by the editor November 20, 2004 and in final revised form October 22, 2005
**Corresponding author

conditions such as minimum temperature T_s and density ρ_s, in the inner part of target configuration called the *hot spark* region must be satisfied.

2. IGNITION PHYSICS

In inertial confinement fusion, a spherical shell of cryogenic deuterium and tritium (DT) filled with DT gas is accelerated by direct laser irradiation (direct drive) or x rays produced by a high-Z enclosure (indirect drive). When an intense laser light is uniformly impinged on a spherical fuel pellet with the intensity of the order of 10^{14}–10^{15} Wcm^{-2}, the laser energy is absorbed on the surface to generate high temperature plasma of 2–3 keV, and an extremely high pressure of a few hundred mega-bars is generated. This pressure accelerates the outer shell of the target towards the target center. The mechanism of the acceleration is the same as rocket propulsion [9]. When the accelerated fuel collides at the center, compression and heating occur. If the dynamics are sufficiently spherically symmetric, the central area is heated up to 5–10 keV (called the 'central spark'), and a fusion reaction starts. In reactor scale implosions, a fuel pellet with an initial radius of about 3mm should be compressed to a radius of about 100 μm. For this purpose, highly precise uniformity is required for irradiation intensity distribution over the fuel pellet, as well as high quality sphericity and uniformity of the fuel pellet. The implosion velocity for achieving the fusion ignition temperature of 5–10 keV at the center is required to be (3-4) × 10^7 cm s^{-1}. Therefore, the pulse length of the laser should be 10–20 ns, and in this time-scale the directed mega-joule energy has to be delivered to a fuel pellet with a radius of about 3 mm [10].

According to isobaric model of fusion targets in inertial confinement fusion, it is assumed that at the final stage of hydrodynamic implosion, target configuration is composed of two distinct regions called *spark* and *cold fuel* [11]. The spark region is an ideal plasma of hydrogen isotopes with density, temperature and a radius of ρ_s, T_s and R_s. On the other hand, cold fuel region is a degenerate electron gas of parameters ρ_c, T_c and R_m, respectively. It is also assumed that pressure is constant across the whole target at stagnation time (maximum compression). This configuration can be generated by a high intensity incident beam of laser or heavy charged particles.

A spark with given values of temperature, T_s, and confinement parameters, $H_s=\rho_s R_s$, can be produced by a hydrodynamic implosion process which then ignites and propagates burning waves in the cold region. Here, there exist processes which cool and dissipate the spark region. Most important of them are bremsstrahlung energy losses of hydrogen isotope plasma and electron thermal conductivity [12].

As a capsule implodes, α-particle deposition from a thermonuclear burn of DT try to heat the central hot spot region. On the other hand, electron conduction from the hot spot to cold surrounding fuel, as well as radiative losses, act to cool the hot spot. If conduction and radiative losses from the hot spot are too large, ignition never occurs. To achieve ignition by the time the implosion process has stopped, the hot spot must have a $\langle \rho r \rangle_{HS}$ equal to about 0.3-0.4 g/cm^2, and must achieve a central temperature of about 5-10 KeV. Under this condition, α-particle energy deposition can overcome losses processes, and a self sustaining burn wave will be generated.

At first, we consider the radiation loss, P_{br}, that is assumed to be bremsstrahlung emission which escapes the fuel power density given by:

$$P_{br} = 5.36\times10^{-24} n_e (n_D + n_T) T_e^{1/2} \qquad erg.\sec^{-1}.cm^{-3} \tag{3}$$

where T_e is electron temperature and n_e, n_D and n_T are electron, deuterium and tritium densities, respectively. Assuming equal number densities ($n_e=n_i=n_s$) and temperatures ($T_e=T_i=T_s$) of electrons and ions in hydrogen plasma we have:

$$P_{br} = 5.36\times10^{-24} n_s^{\,2} T_s^{\,1/2} \qquad erg.\sec^{-1}.cm^{-3} \tag{4}$$

Conduction loss, P_{ec}, is obtained by assuming power law dependence for the heat conduction coefficient and by applying spitzer conductivity [13], (n=5/2) for deuterium-tritium plasma we have:

$$P_{ec} = \xi_{1/2}^2 \kappa_{ec} \frac{KT_s}{R_s^{\,2}} \qquad erg.\sec^{-1}.cm^{-3} \tag{5}$$

here $\xi_{1/2} = 1.3204$ [14], K is the Boltzman constant and κ_{ec} is the electron heat conduction coefficient. The disassembly time of the spark region, t_s, is the time it takes for the sonic motion of ions from the fusion target center to its edge and is given by [15]:

$$t_d = \frac{R_s}{4C_s} \qquad \sec \tag{6}$$

where C_s is sound speed and given by:

$$C_s = \sqrt{\frac{3KT_s}{m_{DT}}} \qquad cm.\sec^{-1} \tag{7}$$

m_{DT} is average atomic weight of equimolar deuterium-tritium mixture. The cooling time scale is evaluated by the following equation:

$$t_c = \frac{3n_s KT_s}{P_{ec} + P_{br}} \qquad \sec \tag{8}$$

For a deuterium-tritium plasma with given values of H_s and T_s, we have a proper spark formation only when the disassembly time scale is smaller or equal to the cooling time scale[16]:

$$t_d \le t_c \tag{9}$$

By substituting corresponding values, an inequality which restricts admissible values of H_s and T_s is formed:

$$8.34\frac{H_s}{T_s} + 6.39\times10^{-3}\frac{T_s^{\,2}}{H_s \ln\Lambda} \le 1 \tag{10}$$

where Coulomb logarithm [13], $\ln\Lambda$, has weak dependence on ρ_s and is given by:

$$\ln\Lambda = \ln\left(60T_s\sqrt{\frac{2.5}{\rho_s}}\right) \tag{11}$$

Now, we introduce a dimensionless parameter which is defined as the ratio of a specific layer to fuel radius at stagnation time that is [17]:

$$\psi = \frac{r}{R_m} \tag{12}$$

above, R_m is fuel external radius at maximum compression time and is a function of isentrope parameter α, implosion velocity U_{im}, spark temperature T_s and fractional spark radius ψ_s, where R_m can be calculated from the energy balance equation. Hence, we would be able to consider the evolution of a class of pellet design with definite values of spark/fuel ratio. So, final expression for the spark formation condition is determined by the following inequality:

$$8.34\frac{H_s}{T_s} + 6.39\times10^{-3}\,\frac{{T_s}^2}{H_s \ln\Lambda} \le 1 \tag{13}$$

We assign $\alpha = 2$ and $\psi_s = 0.5$ as free parameters. The spark formation curves are shown in Fig. 1 for three typical values of implosion velocity (U_{im}=3, 4 and 5 $\times10^7$ cm/sec). These curves form contours that become more compact with implosion velocity increase. In other words, we have spark formation islands where the permissible values of H_s, and T_s lie inside them and show, explicitly, a universal behavior of our graph, giving permissible region of spark temperature and confinement parameter values in the HT plane for the spark formation condition. The upper branches of all curves fully coincide, but its lower branches show a small deviation and open slowly with implosion velocity growth. As seen from Fig. 1, the maximum allowed spark temperature, T_s, decreases with the growth of the implosion velocity and vary from 35 to 26.5 KeV. Therefore, we see that the spark formation curve is not generally affected by implosion velocity.

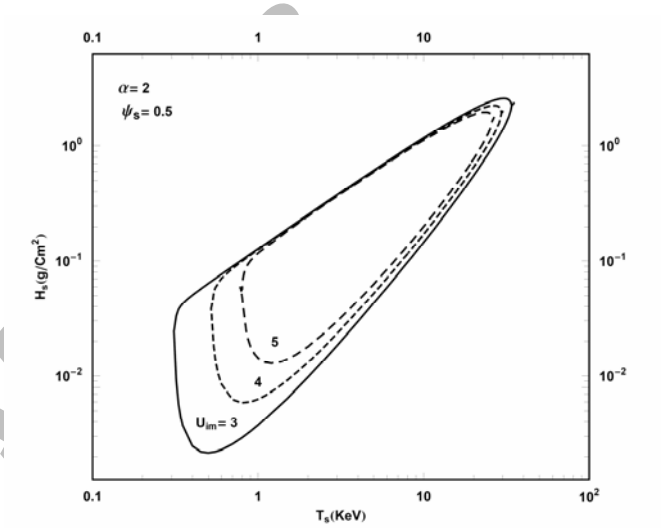

Fig. 1. Spark formation curves with α=2 and ψ_s=0.5 and three different values of implosion velocity in units of 10^7cm/sec

In another step, we must keep in mind that a necessary condition for ignition is that the amount of the energy gain process overcomes loss processes. In our case, this means that the thermonuclear energy release exceed the cooling energy losses process across the spark region.

Thermonuclear heating rate per unit volume and power density are obtained from the burn rate and the fractional alpha particle deposition and is given by:

$$P_{TN} = <\sigma v>_{DT}\, n_D n_T f_\alpha Q_\alpha \qquad erg.\sec^{-1}.cm^{-3} \tag{14}$$

where $\langle\sigma v\rangle_{DT}$ is the Maxwellian averaged fusion rate of a DT mixture [18]:

$$\langle\sigma v\rangle_{DT} = \exp[A_1 + A_2 \,|\ln(T/A_3)|^{A_4}]$$
$$A_1 = -34.629731, \quad A_2 = -0.57164663$$
$$A_3 = 64.221524, \quad A_4 = 2.1373239 \tag{15}$$

f_α is α particle deposition factor, i.e. fraction of alpha particles that remain in the spark region and deposit their energies there. This factor is calculated by solving the transport equation in the approximation of straight trajectories [14]. Also, Q_α is the alpha particle birth energy at the spark center.

So ignition condition can be written as:

$$P_{TN} \geq P_{ec} + P_{br} \tag{16}$$

By substituting corresponding expressions its final form is:

$$\langle\sigma v\rangle_{DT} \frac{H_s}{4} Q_\alpha f_\alpha \geq 5.36\times10^{-24} H_s T_s^{1/2} + 5.109\times10^{-27} \frac{T_s^{7/2}}{H_s \ln\Lambda} \tag{17}$$

The numerical solution of this inequality for three former values of implosion velocity yield curves that determine admissible values of H_s and T_s for spark ignition condition and is shown in Fig. 2. The universal behavior that was mentioned before appears again.

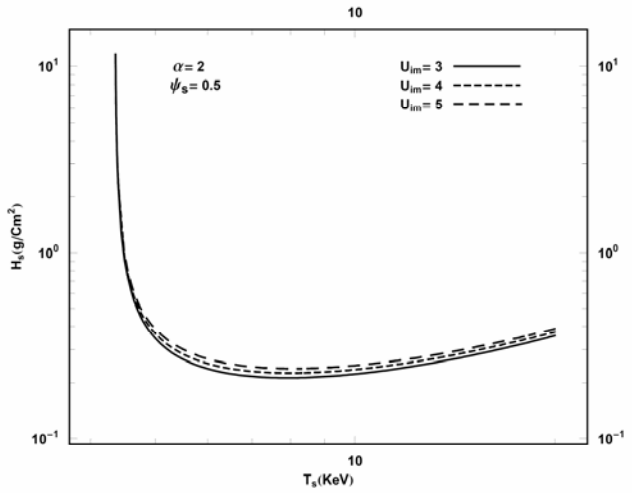

Fig. 2. Spark ignition curves with α=2 and ψ_s=0.5 and three different values of implosion velocity

The left branch of the spark ignition condition curves will also give an important result of the self-ignition temperature. A spark temperature smaller than 5 KeV radiation loss determines the minimum temperature for ignition of 4.4 KeV. However if the pellet is optically thick for an opacity length of λ_a, the pellet has several thickness units from the center to the edge and most of the radiated energy is trapped inside, thus radiation loss is reduced.

Up to now, spark formation and ignition conditions are considered separately. Considering these conditions, simultaneously for a given configuration the restricted region between two curves shows

acceptable values of H_s and T_s, which satisfy our conditions at the same time. This is presented in Fig. 3. The minimum admissible value of spark parameters product is about 1.5 g.cm^{-2}. The KeV that corresponds to the temperature and confinement parameter is $T_s \cong 6.0$ KeV and $H_s \cong 0.25$ g.cm^{-2}, respectively.

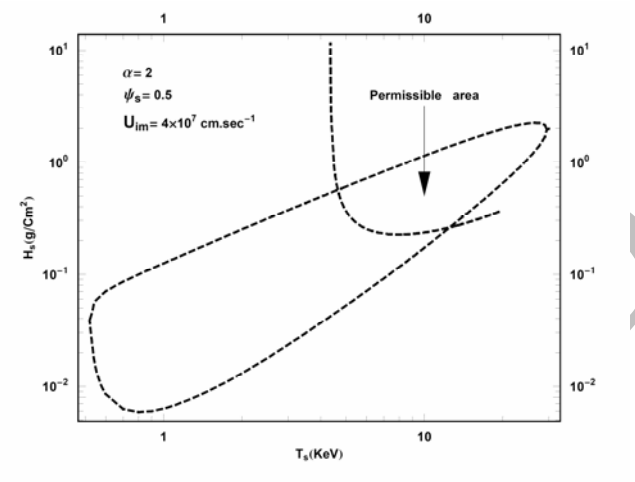

Fig. 3. Spark parameter criteria for a DT pellet parameters with α=2 and ψ_s=0.5 and U_{im}=4×10^{7}cm/sec. Admissible values for H_s, T_s lie between two curves

3. FUEL GAIN MODEL

In this section, we present a simple analytical calculation based on Meyer-Ter-Vehn isobaric model [11] of ICF targets by rewriting all calculations in terms of our dimensionless parameter, ψ_s, and discussing their results. According to this model, it is assumed that compressed DT fuel has a spherical shape of radius R_m (fuel external radius at maximum compression) and step-wise density profile,

$$\rho(r) = \begin{cases} \rho_s, & 0 \le \psi \le \psi_s \\ \rho_c, & \psi_s < \psi \le 1 \end{cases} \tag{18}$$

where $\rho_s < \rho_c$ and Subscripts denote hot spark and cold main fuel regions, respectively. The pressure, P, is constant in the entire fuel volume. Assuming an ideal gas equation of state for the spark region we have:

$$P_s = K' \rho_s T_s \tag{19}$$

where K' *is* constant. On the other hand, adopting a constant value of the isentrope parameter throughout the cold fuel region:

$$\alpha = \frac{P_c}{P_{\deg}} = \frac{(\textit{pressure of main fuel})}{(\textit{Fermi pressure at the density of cold main fuel})} \tag{20}$$

here, P_{deg} is:

$$P_{\deg} = \frac{1}{5}(3\pi^2)^{2/3} \frac{\hbar^2}{m_e} (\frac{\rho_c}{m_{DT}})^{5/3} \tag{21}$$

So, the final expression for pressure balance in compressed fuel is obtained:

$$\mathbf{P} = K'\rho_s T_s = P'\alpha\rho_c^{5/3} \tag{22}$$

here, K' and P' are constants. A schematic diagram of pressure, density and the temperature profile has been shown in Fig. 4. Using Eq. (22), we can easily evaluate spark and fuel region density dependence. So, we have constructed our ignition configuration with five independent parameters H_s (g/cm^2), ψ_s, α, T_s (KeV), and U_{im} (in units of 10^7 cm/sec).

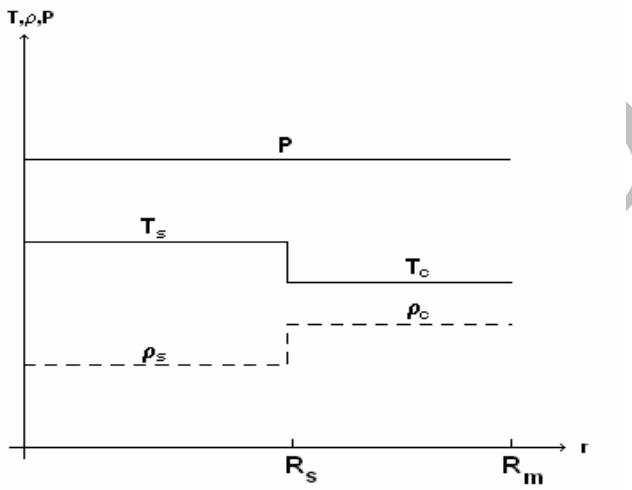

Fig. 4. Schematics of density, temperature, and pressure profiles for isobaric model

Using equation of mass, we have:

$$M_f = \frac{4\pi}{3} R_m^2 [H_s \psi_s^2 + \rho_c R_m (1 - \psi_s^3)] \tag{23}$$

And the following expression for spark cold region energies can be obtained:

$$E_s = H_s T_s R_m^2 \frac{4\pi K \psi_s^2}{m_{DT}} \quad \text{erg} \tag{24}$$

and

$$E_c = 5.18 \times 10^{16} H_s T_s R_m^2 \frac{(1 - \psi_s^3)}{\psi_s} \quad \text{erg} \tag{25}$$

Now, we can use an energy balance equation to obtain an explicit expression for the compressed fuel radius in terms of ignition parameters:

$$\frac{3}{2}\mathbf{P}V = \frac{1}{2} M_f U_{im}^2 \tag{26}$$

Thermonuclear energy gain with respect to energy invested in fuel is calculated as

$$G_f = \frac{E_{TN}}{E_{DT}} = \phi_{DT} f_b \frac{M_f}{E_f} \tag{27}$$

where ϕ_{DT} is the specific DT energy, $3.34\times10^{18}\ erg.g^{-1}$ and f_b are the fraction of burned fuel and in the present work, the following form is used:

$$f_b = [1+(H_B/H_F)]^{-1} = \frac{H_s + \rho_c R_m(1-\psi_s)}{H_s + \rho_c R_m(1-\psi_s) + H_B} \tag{28}$$

where H_B is defined as

$$H_B = \frac{8 m_{DT} C_s}{\langle \sigma v \rangle_{DT}} \tag{29}$$

and is a sensitive function relative temperature variation falling abruptly with an increase in temperature. Since the self heating process causes the temperature to increase up to several 10 KeV, the value of $H_B \cong 7.0\, g.cm^{-2}$ is usually assumed.

The optimum value of fractional spark radius that is obtained is $\psi_s \cong 0.55$, which is different with its corresponding value in the Basko self-similar model. This discrepancy essentially occurs because of a more realistic pressure profile across cold fuel in the Basko model. It also tells us about the most economical regime of ignition, where maximum fuel mass can be ignited by a given ignition energy [14] and is shown in Fig. 5.

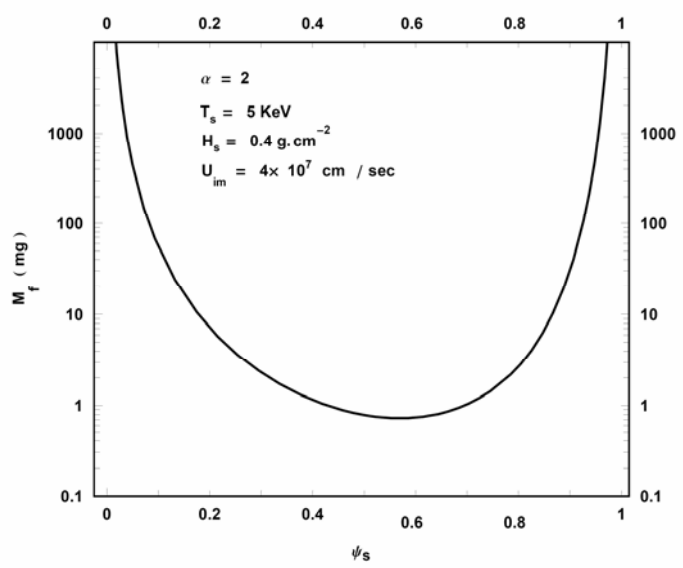

Fig. 5. Fuel mass as a function of ψ_s for fixed values of H_s, T_s, α=2 and U_{im}

4. LIMITING GAIN CURVE

The question of the required amount of energy for a proper ignition of a fusion capsule is one of the aims in ICF research and has considerable importance in the optimization of target design and drivers (lasers or accelerators) , since we want to reach the highest value of energy gain with a given driver energy, $G_f(E_{dr})$.

In a recent publication [19, 20] the dependence of target energy gain, G_T [$G_T(E_{dr}) = \eta_H G_f(E_f)$], on the driver energy, E_{dr}, has been discussed with a family of gain curves corresponding to different values of implosion velocity, U_{im}. So, if we have two systems in which their parameters are scaled

relative to each other with a scale factor of ξ , we have the following relations between scaled and parent systems:

$$r' = \xi r\,, \quad M' = \xi^3 M\,, \quad E' = \xi^3 E \tag{30}$$

where prime denote parameters in the scaled system. If, however, velocity, temperature and density remained fixed:

$$U' = \sqrt{\frac{E'}{M'}} = U\,, \quad \rho' = M'/r'^3 = \rho\,, \quad T' = E'/M' = T \quad I' = \frac{1}{r'^3}\sqrt{\frac{E'^3}{M'}} = I \tag{31}$$

If we obey these relations in our design, the capsule implodes along the same sequence of state in the ρ, T plane and reaches the same implosion velocity and the same maximum density and temperature at the time of maximum compression. The implosion velocity that is scaled in this way, preserves the values of capsule instability parameters [14]. Hence, a gain curve that was obtained for a given value of implosion velocity represents a class of capsule design with different sizes. Any such curve has an ignition threshold, $E_{dr,\,min}$, since for a given implosion velocity, U_{im}, arbitrary fuel masses for ignition is not allowed. The envelope of gain curves for different implosion velocity is the limiting (fuel) gain curve, (G_f*) G_T*.

In recent years, some authors [14, 19 and 20] have done various complex calculations to present the ignition energy scaling (E_{ign}) relations relative to various parameters of capsule implosion. Thus, Scaling relation in ICF research has critical importance both scientifically and economically.

If we plot fuel gain as a function of ignition energy for fixed implosion velocity and limited values of spark fractional radius $0.1<\psi_s<0.8$, we will obtain a series of gain curves. The envelope of these gain curves has been shown with a dash line G_f* and is proportional to $E_f^{0.32}$, which is calculated numerically and is shown in Fig. 6. This result is in good agreement with one that was obtained by Basko by a self-similar solution of hydrodynamics equations for a bare DT sphere in its simple approximation without any additional constraints.

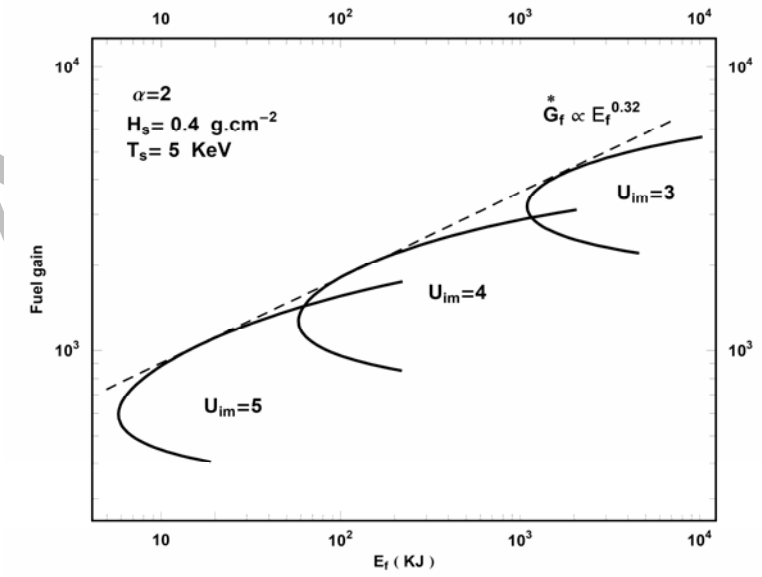

Fig. 6. Fuel gain curves (full lines) and limiting fuel gain curve (dash line) as a function of compressed fuel energy. The gain curves are obtained by varying $0.1<\psi_s<0.8$ for isentrope $\alpha=2$

5. CONCLUSIONS

In this paper, it is shown that for ICF targets considered with cooling processes, a limited set of $\{H_s, T_s\}$ values are obtained which simultaneously satisfy formation and ignition conditions. These graphs have a free implosion velocity behavior and remain fixed relative to their variations, and hence give universal admissible values of spark parameters. Therefore, by growth of implosion velocity, the maximum permissible values of the spark temperature decrease. For a typical implosion velocity, its average maximum value is about 30 KeV.

Also, fuel energy gain curves as a function of fuel energy for different implosion velocity is plotted and the envelope of the gain curves was calculated numerically, showing good consistency with the one obtained by Basko [14], since the nature of the two calculations are the same, but have a small difference in details due to some realistic assumptions about pressure, density and temperature profiles of compressed fuel at ignition time.

REFERENCES

1. Yamanaka, C. (1999). Inertial fusion research over the past 30 years. *Fusion Engineering and Design*. *44*, 1.
2. Wootton, A. J. & Perkins, L. J. (2000). Issues for magnetic and inertial fusion energy development. *Plasma Phys. Control. Fusion*, *42*(B1), 25.
3. Nuckolls, H. J., Wood, L., Thiessen, A. & Zimmerman, G. B. (1972). Laser compression of matter to super-high densities: thermonuclear (CTR) applications. *Nature*. *239*, 129.
4. Brueckner, K. A. & Jorna, S. (1974). Laser-driven fusion, *Rev. Mod. Phys*. *46*, 325.
5. Lindl, J. D., McCory, R. L. & Campbell, E. M. (1992). Progress toward ignition and burn propagation in inertial confinement fusion. *Phys. Today*. *45*, 32.
6. Basko, M. M. (2003). New developments in the theory of ICF targets, and fast ignition with heavy ions. *Plasma Phys. Control. Fusion*. *45*(A1), 25.
7. Mason, R. J. & Morse, R. L. (1975). Hydrodynamics and burn of optimally imploded deuterium-tritium spheres. *Phys. Fluids*. *18*, 814.
8. Nuckolls, J. H. (1982). The feasibility of inertial-confinement fusion, *Phys. Today*. 35, 24.
9. Nakai, S. & Mima, K. (2004). Laser driven inertial fusion energy: present and prospective. *Rep. Prog. Phys*. *67*, 321.
10. Nakai, S. & Takabe, H. (1996). Principles of inertial confinement fusion physics of implosion and the concept of inertial fusion energy. *Rep. Prog. Phys*. *59*, 1071.
11. Meyer-Ter-vehn, J. (1982). On energy gain of fusion targets: The model of kidder and bodner improved. *Nucl. Fusion*. *22*, 561.
12. Ghasemizad, A. & Khoshbinfar, S. (2004). The central spark ignition, A way toward clean fuels in nuclear energy and environment, *5th International Conference on Nuclear Option in countries with Small and Medium Electricity Grids*, (16-20). Dubrovnik, Croatia.
13. Spitzer, L. (1956). *Physics of fully ionized gases*. London, Inter-science Publ.
14. Basko, M. M. (1995). On the scaling of the energy gain of ICF targets. *Nucl. Fusion*. *35*, 87.
15. Eskandari, M. R. (1995). Principle of nuclear fusion. *Shiraz University publishing center*.
16. Basko, M. M. (1990). Spark and volume ignition of DT and D_2 microsphere. *Nucl. Fusion*. *30*, 2443.
17. Choudhauri, A. (1999). *The physics of fluids and plasmas*. Cambridge University press.
18. Piriz, A. R. (1996). Conditions for the ignition of imploding spherical shell targets. *Nuclear Fusion*. *36*, 1395.

19. Murakami, M. & Iida, D. (2002). Scaling laws for hydrodynamically similar implosions with heat conduction. *Phys. Plasmas*. *9*, 2745.
20. Herrmann, M. C., Tabak, M. & Lindl, J. D. (2001). A generalized scaling law for the ignition energy of inertial confinement fusion capsules. *Nucl. Fusion*. *41*, 99.